

EFFECTIVE MODE-II STRESS INTENSITY FACTOR FOR PARTIALLY OPENED NATURAL CRACKS UNDER MIXED-MODE LOADING

T. Fett

Institut für Materialforschung II, Forschungszentrum Karlsruhe,
Postfach 3640, 76021 Karlsruhe, Germany

ABSTRACT

Failure considerations under mixed-mode loading need knowledge about the influence of friction between partially closed crack faces in the case of a negative mode-I stress intensity factor. A simple relation is derived, which enables to compute friction contributions to the mode-II stress intensity factor K_{II} for the case of negative mode-I stress intensity factors K_I . The relation is exact for the limit case of an edge crack in a half-space. It can be shown that an adequate description of small natural cracks is possible. The effective stress intensity factor is computed for a contact loading problem between a flat bar and cylinders.

KEYWORDS

Crack closure, effective stress intensity factor, friction, mixed-mode loading.

INTRODUCTION

Under mixed-mode loading failure of a crack-containing component occurs, if a function f of the three stress intensity factors reaches a critical value f_c

$$f(K_I, K_{II}, K_{III}) = f_c \quad (1)$$

Several mixed-mode fracture criteria have been proposed. In most commonly used criteria only K_I and K_{II} are included in the function f . The most popular failure criterion is that of the coplanar energy release rate [1]. Under plane strain conditions it reads

$$\sqrt{K_I^2 + K_{II}^2 + \frac{1}{1-\nu} K_{III}^2} = K_{Ic} \quad (2)$$

This criterion makes sense only for positive K_I . For $K_I < 0$ the crack faces are under compression and no singular mode-I stress field exists. Nevertheless, a mode-II stress intensity factor can occur, caused by the superimposed shear loading. Due to friction between the crack faces, K_{II} has to be calculated with an effective shear stress [2].

$$\tau_{\text{eff}} = \begin{cases} \tau & \text{for } \sigma_n > 0 \\ |\tau| + \mu\sigma_n & \text{for } |\mu\sigma_n| < |\tau| \\ 0 & \text{for } |\mu\sigma_n| > |\tau| \end{cases} \quad (3)$$

If the considered crack is small compared with the variation of normal stresses σ_n (i.e. if the effective shear stress is sufficiently constant over the crack size) it holds simply

$$K_{II} = \tau_{\text{eff}} Y \sqrt{a} \quad (4)$$

with the geometric function Y for constant shear stresses. Equation (4) is correct only for cracks with completely closed crack faces. The aim of the contribution is to compute the effective stress intensity factor also for partially closed cracks.

STRESS INTENSITY FACTORS FOR STRONGLY VARYING STRESSES

In the case of a crack size comparable to the variation length of normal stresses, the computation becomes more complex. Stresses with very strong gradients predominantly occur near contact loads. Figure 1a shows a rectangular bar symmetrically loaded by a pair of forces P acting via two cylinders. At the distance x from the symmetry line an edge crack of depth a is assumed to exist. The stresses occurring in the uncracked bar can be computed from [3]. The stress distributions along the cross section AA (Fig. 1a) are plotted in Figs. 1b and 1c for a contact width of $s/H=0.1$, normalised on

$$\sigma^* = P/(HB) \quad (5)$$

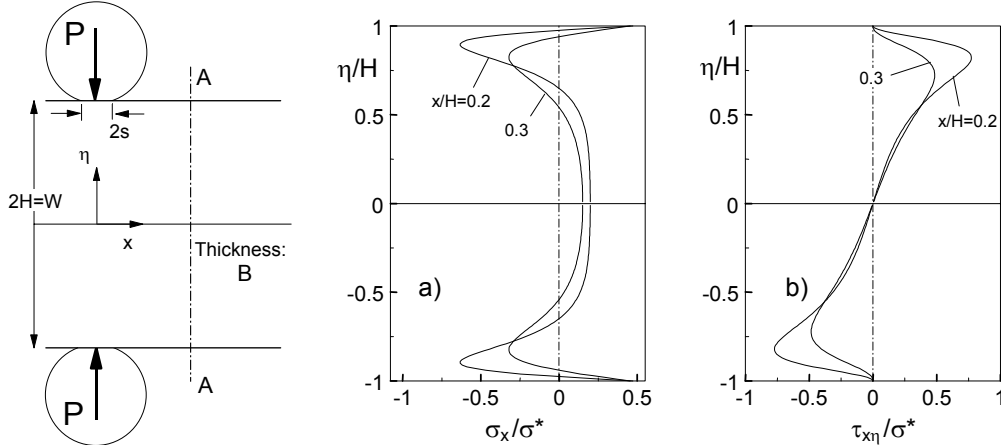


Figure 1: a) Geometric data for a bar loaded by two opposed cylinders, b) stress normal to cross section AA, c) shear stress in cross section AA.

COMPUTATION OF STRESS INTENSITY FACTORS

Natural surface cracks in ceramics are often modelled as edge cracks. An edge crack at the free surface of depth a orientated in y -direction is considered in Fig. 2a. From the stresses, present in the uncracked body, the applied stress intensity factors $K_{I,appl}$ and $K_{II,appl}$ can be computed according to [4]

$$K_{\text{appl},I} = \int_0^a h_I(y, a) \sigma_x(y) dy \quad (6)$$

$$K_{\text{appl},II} = \int_0^a h_{II}(y, a) \tau_{xy}(y) dy \quad (7)$$

with the weight functions h_I for mode-I and h_{II} for mode-II loading. The results obtained with the weight function solutions given in [5] are plotted in Figs. 2a and 2b.

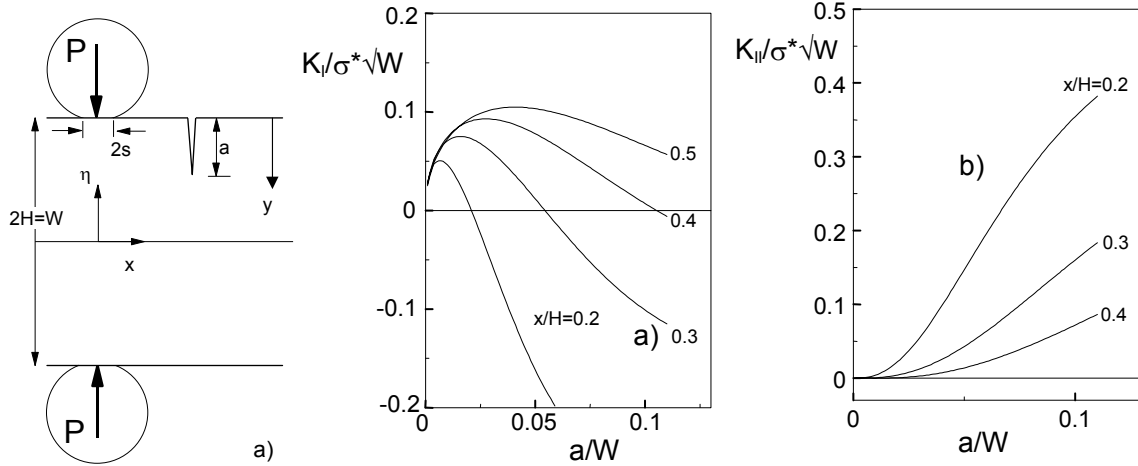


Figure 2: Stress intensity factors for edge cracks, a) mode-I and b) mode-II stress intensity factor.

From this representation it is obvious that the mode-I stress intensity factors are first positive due to the tensile stresses near the free surface ($\eta/H \rightarrow 1$ in Fig 1b) and then become negative at larger depths. In this case at least partial crack closure must occur. In order to predict failure by the remaining stress intensity factor K_{II} , it is necessary to determine that mode-II stress intensity factor contribution which reduces the applied stress intensity factor by crack surface friction.

Figure 3a shows the crack opening displacement δ_{appl} resulting from the applied stress $\sigma_{appl} = \sigma_x$. The penetration of the crack faces reflects the negative mode-I stress intensity factor. In a real structure crack-face penetration is not possible of course. The crack faces are in direct contact, producing contact stresses σ_{cont} as illustrated in Fig. 3b.

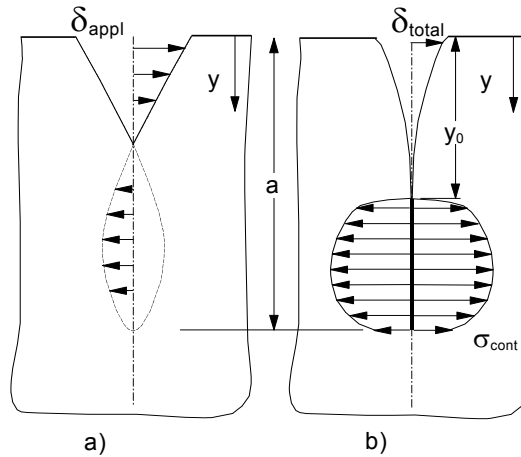


Figure 3: Schematic illustration of stresses and displacements: a) crack opening displacements from applied stresses (penetration allowed), b) crack closure and resulting contact stresses.

In the region where the crack is closed it holds

$$\delta_{total} = \delta_{appl} + \delta_{cont} = 0 \quad \text{for} \quad y_0 \leq y \leq a \quad (8)$$

The near-tip displacement must vanish, i.e.

$$\lim_{y \rightarrow a} \delta_{total} = \sqrt{\frac{8}{\pi}} \frac{K_{total}}{E'} \sqrt{a - y} \quad (9)$$

and, consequently, the total stress intensity factor must disappear, too

$$K_{I,total} = K_{I,appl} + K_{I,cont} = 0 \quad (10)$$

In weight function representation Eqn.(10) reads

$$K_{I,total} = \int_0^a h_I(y, a) \sigma_n(y) dy + \int_{y_0}^a h_I(y, a) \sigma_{cont}(y) dy = 0 \quad (11)$$

Due to the contact stresses σ_{cont} between the crack surfaces, friction is caused, resulting in a mode-II stress intensity factor contribution $K_{II,frict}$

$$K_{II,frict} = -\mu \int_{y_0}^a h_{II}(y, a) \sigma_{cont}(y) dy, \quad K_{I,appl} \leq 0 \quad (12)$$

where μ is the friction coefficient. Then the effective mode-II contribution is

$$K_{II,eff} = K_{II,appl} + K_{II,frict} \quad (13)$$

Numerical evaluation of the contact stresses needs the solution of the integral equation [5]

$$\delta_{total}(y) \times E' = \int_y^a h(y, a') \left[\int_0^{a'} h_I(y', a') \sigma_{appl}(y') dy' + \int_{y_0}^{a'} h_I(y', a) \sigma_{cont}(y') dy' \right] da' \quad (14a)$$

$$\text{with} \quad \delta_{total}(y) = 0 \quad \text{for} \quad y \leq y_0 \leq a \quad (14b)$$

In Eqn.(14a) E' is the plane strain Young's modulus. From the solution of the integral equation (14) the distributions of the contact stresses $\sigma_{cont}(y)$ and total displacements $\delta_{total}(y)$ are obtained. The solution of (14) can be determined by several numerical methods, for instance by the "iterative approximation". As an additional condition $d\delta_{total}/dy = 0$ for $y = y_0$ has to be satisfied. In Fig. 4 all displacement contributions are plotted for arbitrarily chosen values of y_0/W . The additional condition for the total displacements ($d\delta_{total}/dy = 0$ for $y = y_0$) is fulfilled here for $y_0/a \approx 0.7$, i.e. the correct solution is obtained for this y_0/W .

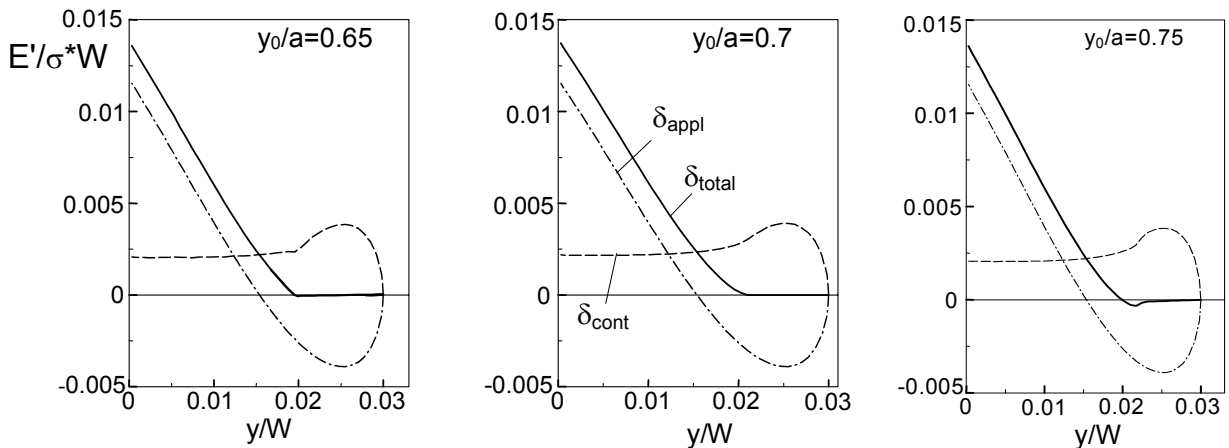


Figure 4: Displacements for a crack of depth $a/W = 0.03$ and differently chosen y_0/a .

The related contact stress distribution is plotted in Fig. 5a. From Eqn.(12) the friction part $K_{II,frict}$ and from Eqn.(13) the effective mode-II stress intensity factor can be determined. In Fig. 5b the friction stress intensity factor $K_{II,frict}$ (solid curve) is shown together with the applied stress intensity factor $K_{I,appl}$ (dashed curve). The two curves show a very good agreement for $0.02 < a/W < 0.06$, i.e. $K_{II,frict} \cong K_{I,appl}$.

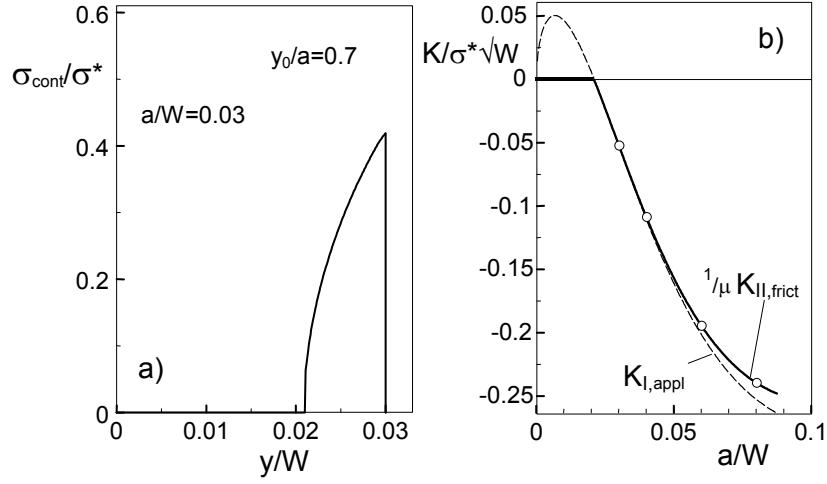


Figure 5: a) Distribution of contact stresses σ_{cont} , b) friction stress intensity factor $K_{II,frict}$ for $x/H=0.2$.

EFFECTIVE K_{II} FOR SMALL CRACKS

Determination of the friction stress intensity factor is relatively complicated since it needs the solution of an integral equation. A useful approximation will be derived below. From Eqn.(11) it results

$$\int_{y_0}^a h_I(y, a) \sigma_{cont}(y) dy = -K_{I,appl} \quad (15)$$

For the evaluation of Eqn.(12) we need a very similar integral, namely

$$I = \int_{y_0}^a h_{II}(y, a) \sigma_{cont}(y) dy \quad (16)$$

Now let us use the fact that in the limit case $a/W \rightarrow 0$ (i.e. for very small cracks) the mode-I and mode-II weight functions are identical. Then, combining Eqs.(12), (15), and (16) provides the simple result of

$$K_{II,frict} = \mu K_{I,appl} \quad \text{for } K_{I,appl} \leq 0 \quad (17)$$

Having this result in mind, we can conclude that the agreement of the two curves in Fig. 5b is not a feature of the specially chosen stress distribution.

In order to estimate the errors made by application of Eqn.(17) to larger cracks, one has to look for the deviations between h_I and h_{II} . In Fig. 6a the two weight functions proposed in [6] are plotted for several relative crack depths a/W . Figure 6b shows the ratio h_I/h_{II} . The crack depths of natural cracks in ceramic materials are in the order of $50 \mu\text{m}$, the widths of commonly used test specimens are $> 3\text{mm}$ in most cases. The relative crack size for standard tests therefore is $a/W < 0.02$. For cracks in this range of relative depths the maximum deviations between the two weight functions are less than 2%. The maximum deviations of the stress intensity factors are, of course, less than the maximum deviations of the weight functions. This is due to the integration of the weight function over a positive stress, by which the curves in Fig. 6b are averaged as a consequence of the mean value theorem for integrals.

The effective stress intensity factor K_{eff} , combining K_I and K_{II} , was computed by

$$K_{eff} = \begin{cases} \sqrt{K_I^2 + K_{II}^2} & \text{for } K_I > 0 \\ K_{II} + \mu K_I & \text{for } K_I < 0 \end{cases} \quad (18)$$

and is represented in Fig. 7. The coefficient μ was chosen as $\mu = 0.5$. At the crack depth for which $K_I = 0$ is fulfilled, the resulting K_{eff} is continuous but not smooth.

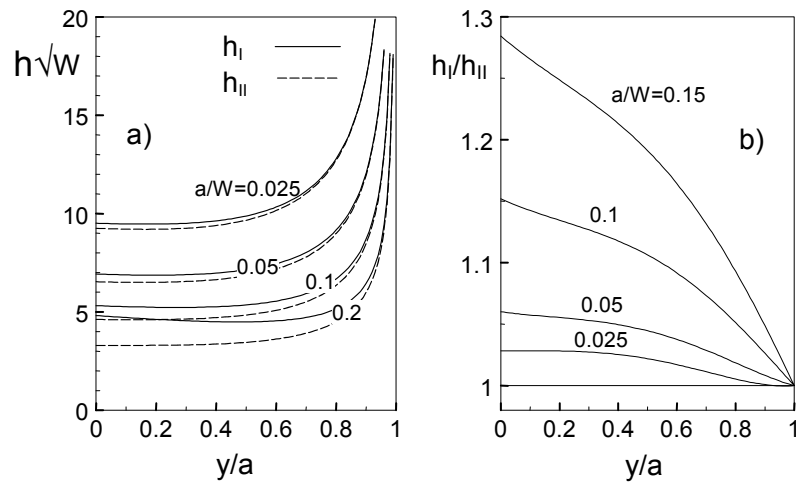


Figure 6: Comparison of the mode-I and mode-II weight functions.

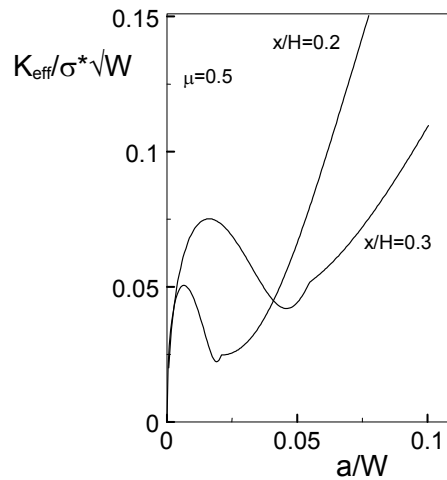


Fig. 7 Effective stress intensity factors for edge cracks perpendicular to the free surface at several distances from the load application cylinders.

References

1. Paris, P.C., Sih, G.C. (1965), ASTM STP **381**, 30–80.
2. Alpa, G. (1984) *Engng. Fract. Mech.* 19, 881–901.
3. Fett, T., Munz, D., Thun, G. (2001). *Journal of Testing and Evaluation*.
4. Bueckner, H. (1979). *ZAMM* 50, 529–546
5. Munz, D., Fett, T. (1999). *CERAMICS, Failure, Material Selection, Design*, Springer-Verlag, Heidelberg
6. Fett, T., Munz, D. (1997). *Stress Intensity Factors and Weight Functions*, Computational Mechanics Publications, Southampton, UK